Structural Analysis of Interactions for Complex Formation between Ferredoxin-NADP$^+$ Reductase and Its Protein Partners

Tomás Mayoral,[1] Marta Martínez-Júlvez,[2] Inmaculada Pérez-Dorado,[1] Julia Sanz-Aparicio,[1] Carlos Gómez-Moreno,[2] Milagros Medina,[2] and Juan A. Hermoso[1]*

[1]*Grupo de Cristalografía Macromolecular y Biología Estructural, Instituto Química-Física Rocasolano, C.S.I.C. Serrano 119, 28006-Madrid, Spain*

[2]*Departamento de Bioquímica y Biología Molecular y Celular and Institute of Biocomputation and Physics of Complex Systems (BiFi), Facultad de Ciencias, Universidad de Zaragoza, 50009-Zaragoza, Spain*

ABSTRACT **The three-dimensional structures of K72E, K75R, K75S, K75Q, and K75E *Anabaena* Ferredoxin-NADP$^+$ reductase (FNR) mutants have been solved, and particular structural details of these mutants have been used to assess the role played by residues 72 and 75 in optimal complex formation and electron transfer (ET) between FNR and its protein redox partners Ferredoxin (Fd) and Flavodoxin (Fld). Additionally, because there is no structural information available on the interaction between FNR and Fld, a model for the FNR:Fld complex has also been produced based on the previously reported crystal structures and on that of the rat Cytochrome P450 reductase (CPR), onto which FNR and Fld have been structurally aligned, and those reported for the *Anabaena* and maize FNR:Fd complexes. The model suggests putative electrostatic and hydrophobic interactions between residues on the FNR and Fld surfaces at the complex interface and provides an adequate orientation and distance between the FAD and FMN redox centers for efficient ET without the presence of any other molecule as electron carrier. Thus, the models now available for the FNR:Fd and FNR:Fld interactions and the structures presented here for the mutants at K72 and K75 in *Anabaena* FNR have been evaluated in light of previous biochemical data. These structures confirm the key participation of residue K75 and K72 in complex formation with both Fd and Fld. The drastic effect in FNR activity produced by replacement of K75 by Glu in the K75E FNR variant is explained not only by the observed changes in the charge distribution on the surface of the K75E FNR mutant, but also by the formation of a salt bridge interaction between E75 and K72 that simultaneously "neutralizes" two essential positive charged side chains for Fld/Fd recognition. Proteins 2005;59:592–602.**

Key words: complex formation; electrostatic interactions; Ferredoxin; Flavodoxin; Ferredoxin-NADP$^+$ reductase

INTRODUCTION

Electron transfer (ET) reactions between proteins are key processes in many biological systems. These reactions require formation of a complex that allows the optimal orientation between the redox centers for the subsequent ET. This is the case of the ET chain that addresses electrons from Photosystem I (PSI) to FNR to reduce NADP$^+$ to NADPH during the photosynthesis. In this system, the flavin-dependent Ferredoxin-NADP$^+$ reductase (FNR) catalyses the transfer of two electrons from two independent Ferredoxin (Fd) molecules, previously reduced by PSI, to NADP$^+$ according to the reaction:[1,2]

$$2Fd_{rd} + NADP^+ + H^+ \rightarrow 2Fd_{ox} + NADPH$$

In the case of some algae and cyanobacteria, under iron-deficient conditions, an FMN-dependent protein, Flavodoxin (Fld), replaces Fd in the ET from PSI to FNR.[3,4] Thus, despite their differences in folding, size, and redox cofactor, Fd and Fld apparently play the same role in the ET from PSI to FNR.

The three-dimensional structure of FNR has been proposed to be the prototype of a family of flavin-dependent reductases that function as transducers between pyridine nucleotides (two electron carriers) and different one-electron carriers.[5–8] Its polypeptidic chain is folded in two domains: the FAD-binding domain (residues 1–138, *Anabaena* numbering), and the NADP$^+$-binding domain (residues 139–303). The FAD-binding domain is made up of a scaffold of six antiparallel strands arranged in two perpendicular β-sheets, whereas the NADP$^+$ binding do-

Abbreviations: CPR, cytochrome-P450 reductase; ET, electron transfer; Fd, ferredoxin; Fd_{ox}, Fd in the oxidized state; Fd_{rd}, Fd in the reduced state; Fld, flavodoxin; FNR, ferredoxin-NADP$^+$ reductase.

Grant sponsor: Comisión Interministerial de Ciencia y Tecnología (CICYT); Grant numbers: BIO2003-0627 (to C.G.-M.) and BIO2004-00279 (to M.M).

*Correspondence to: Juan A. Hermoso, Grupo de Cristalografía Macromolecular y Biología Estructural, Instituto Química-Física Rocasolano, C.S.I.C. Serrano 119, 28006-Madrid, Spain. E-mail: xjuan@iqfr.csic.es

Received 21 July 2004; Accepted 12 November 2004

Published online 23 March 2005 in Wiley InterScience (www.interscience.wiley.com). DOI: 10.1002/prot.20450

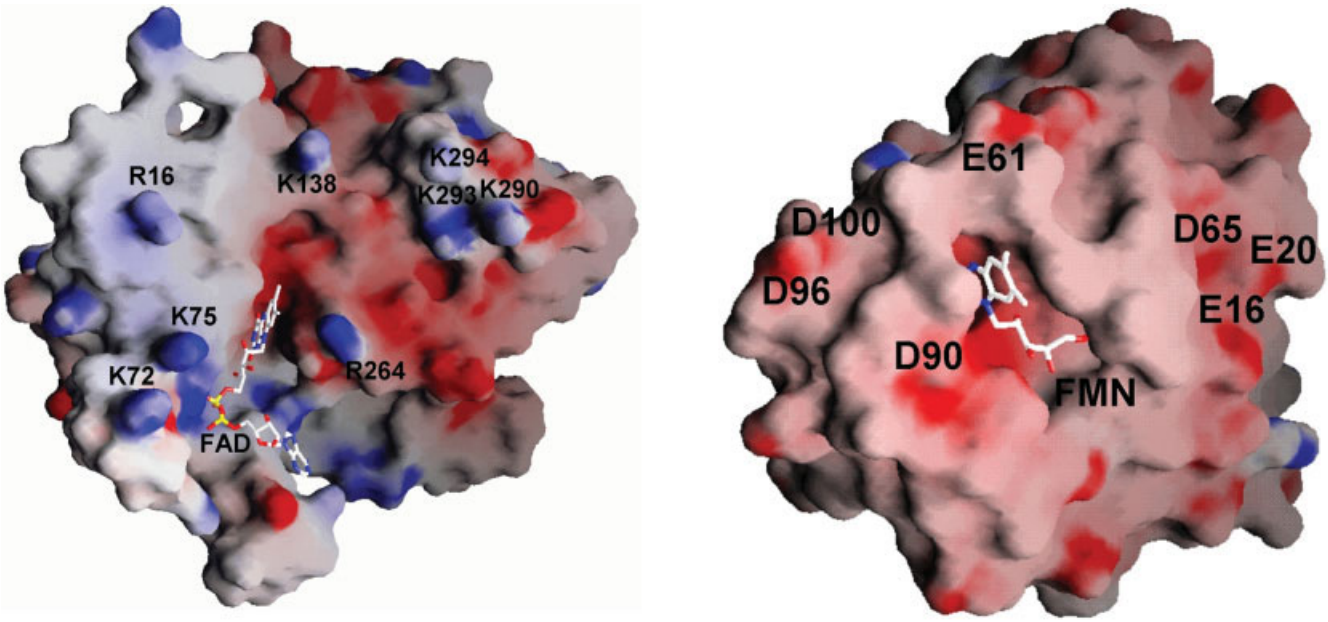

Fig. 1. Molecular surface showing the electrostatic potentials of (A) WT FNR and (B) WT Fld. Positive charges are shown in blue and negative ones in red. The FAD and FMN cofactors are represented as sticks.

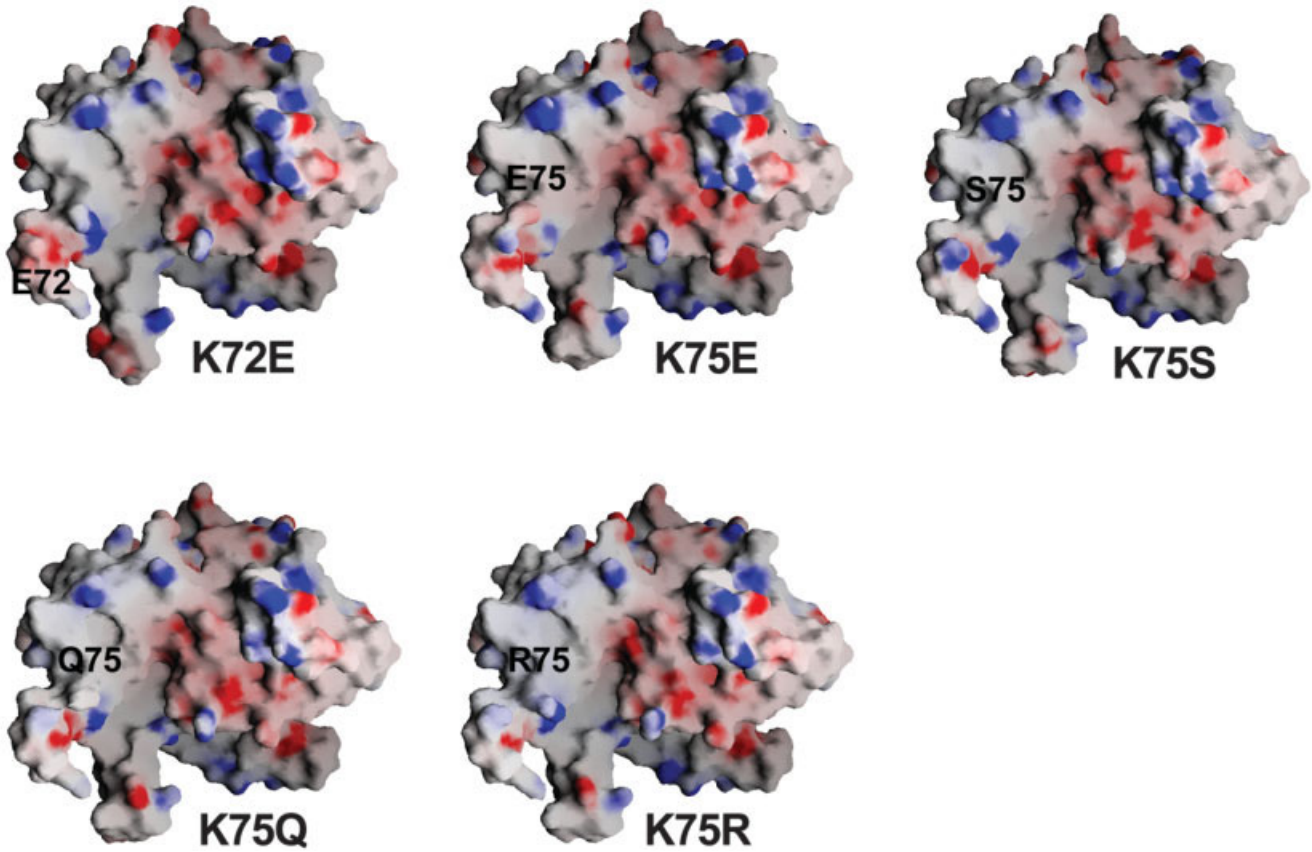

Fig. 2. Molecular surface representations of mutated FNRs showing their electrostatic potentials and mutated positions.

main shows a characteristic fold of nicotinamide dinucleotide binding enzymes with five parallel β-strands surrounded by seven α-helices. Between both domains, there is a very noticeable cavity where Fd and Fld are proposed to bind.[7–11] Fd presents 98 residues folded in four β-strands surrounded by three short α-helices and a [2S-2Fe] center

TABLE I. Steady-State Kinetics Parameters of WT and Mutated *Anabaena* FNR Forms in the NADPH-Dependent Cytochrome *c* Reductase Activity[a] and Dissociation Constant Measurements with Fd and Fld[b]

	NADPH-dependent cytochrome *c* reductase activity						Dissociation constants	
	With ferredoxin			With flavodoxin				
FNR	k_{cat} (s^{-1})	K_m^{Fd} (μM)	k_{cat}/K_m^{Fd} ($\mu M^{-1}s^{-1}$)	k_{cat} (s^{-1})	K_m^{Fld} (μM)	k_{cat}/K_m^{Fld} ($\mu M^{-1}s^{-1}$)	FNR_{ox}:Fd_{ox} K_d^{Fd} (μM)	FNR_{ox}:Fld_{ox}[i] K_d^{Fld} (μM)
WT[c]	200	11	18.2	23.3	33	0.70	4	3
R16E[d]	110	>500	<0.22	10.2	>500	0.02	120	n.d.
K72E[d]	233	>500	<0.47	7.8	283	0.03	50	n.d.
K75R[e]	270	94	2.9	23.3	15	1.6	4.8	n.d.
K75Q[e]	190	>500	<0.38	27	632	0.042	380	n.d.
K75S[e]	200	>500	<0.4	50	800	0.062	200	n.d.
K75E[e]	—[g]	—	—	—[g]	—	—	n.d.[h]	n.d.
K138E[d]	106	187	0.57	11.7	310	0.040	4.1	n.d.
R264E[f]	200	212	0.98	21.6	544	0.040	3.3	9.4
K290E[d]	180	218	0.83	25	183	0.14	4.0	7.1
K294E[d]	252	208	1.22	15.8	125	0.13	7.2	20.3

[a]This activity was assayed in 50 m*M* Tris/HCl, pH 8.0 using either Fd or Fld as electron carrier from FNR_{rd} to cytocrome *c* at 25°C as described in Ref 46.
[b]K_d values of the complexes between oxidised FNR mutants and either oxidised Fd or Fld were measured by differential spectroscopy in 50 mM Tris/HCl, pH 8.0 at 25°C as previously described in Ref. 46.
[c]Taken from Ref. 46.
[d]Taken from Ref. 10.
[e]Taken from Ref. 30.
[f]Taken from Ref. 25.
[g]No shown activity of K75E with Fd or with Fld.
[h]The spectral perturbation due to the binding was too weak to be measured.
[i]The K_d value could be measured only in three cases: R264E, K290E, and K294E.

as the redox cofactor,[12] whereas Fld is formed by 169 residues folded in a five parallel β-strand central core surrounded by five α-helices[13] and contains a noncovalently bound FMN cofactor as the redox center [Fig. 1(A)]. Several approaches have been followed to study the processes of recognition and the subsequent ET between FNR and its protein redox partners (Fd/Fld). Today, it is accepted that not only electrostatic but also hydrophobic forces are involved in achieving the optimal interaction between FNR and Fd, or Fld, for efficient ET.[9,10,14–27] Thus, positively charged residues on FNR [Fig. 1(A)] and negative ones on the protein partner, Fd or Fld [Fig. 1(B)], have been shown to be involved in the initial approximation of proteins for complex formation, whereas both charged and hydrophobic side chains have been shown to be critical in the stabilization of the optimal complex for ET. Crystal structures have been reported for the FNR:Fd complexes from *Anabaena*[11] and maize,[32] allowing to extend our knowledge of the interaction surface between these two proteins. However, no three-dimensional model for the FNR:Fld interaction is available.

Among the charged side chains on the molecular FNR surface, R16, K72 and, especially K75 (K88 in spinach), have been proven to be crucial for efficient interaction with Fd and Fld.[10,23,29–31] Positions K72 and K75 of *Anabaena* FNR are highly conserved in FNR sequences from different species (see Table 1 in Ref. 30), being located on the enzyme surface, with no intramolecular interactions and near the cavity where the pyrophosphate and the ribose moieties of the FAD are located [Fig. 1(A)]. Conservative replacement of K75 produced an enzyme of identical behavior than WT FNR, whereas replacement by Gln or Ser induces the destabilization of the protein–protein interaction, although this does not affect the ET itself (Table I). Finally, introduction of a negative charge either at position K72, or especially, at position K75, drastically impairs complex formation with Fd and Fld and, consequently, ET (Table I). Contribution of the K75 side chain to the modulation of the FAD reduction potential within the FNR environment has also been postulated, because replacement of K75 by a Glu makes $E_{ox/sq}$ less negative by −20 mV.[31]

In the three-dimensional structures reported for the FNR:Fd interaction well-defined salt bridges can be observed between Nξ of K75 FNR (K91 in maize) and Oξ2 of the E94 Fd negative side chain (D65 in maize).[11,33] To obtain further knowledge of the interaction and ET of FNR with its protein partners, in the present work the three-dimensional structures of different *Anabaena* FNR mutants at positions K72 and K75 (namely: K72E, K75R, K75Q, K75S, and K75E) have been solved, and a model for the three-dimensional structure for the FNR:Fld interaction produced based on the structure of the rat microsomal Cytochrome P450 reductase (CPR).[33] This reductase is involved in the oxidative metabolism of both endogenous and exogenous compounds including therapeutic drugs and other environmental toxicants and carcinogens, belongs to the FNR family, and contains an FNR-like module with FAD as the cofactor connected, through the same polypeptide chain, to an FMN domain. Moreover, the FMN-binding domain of microsomal CPR is also similar to Fld. Therefore, the CPR resemblance to the algal and

TABLE II. Data Collection and Refinement Statistics

Mutant	K72E	K75E	K75Q	K75R	K75S
Temperature (K)	100	100	100	100	100
X-ray source	Synchrotron	Synchrotron	Rotating-anode	Rotating-anode	Rotating-anode
Space group	$P6_5$	$P6_5$	$P6_5$	$P6_5$	$P6_5$
Cell a,b,c (Å)	86.64;86.64;96.27	87.00;87.00;96.70	88.18;88.18;97.20	88.10;88.10;97.17	88.13;88.13;97.23
Resolution range (Å)	22.2–1.7	22.2–1.7	35.5–2.3	35.5–2.3	35.5–2.3
No. of unique refl.	43287	37317	18870	18750	18682
Completeness of data (%)	98.0	86.6	99.3	99.4	99.2
R_{sym} [a] (%)	0.051	0.051	0.101	0.103	0.08
Refinements Statistics					
Resolution range (Å)	10.0–1.7	9.0–1.7	15.0–2.3	15.0–2.3	15.0–2.3
No. of protein atoms	2338	2338	2340	2335	2338
No. of heterogen atoms	58	58	58	58	58
No. of solvent atoms	306	500	154	221	174
R_{factor} [b] (%)	22.7	20.8	20.0	19.0	19.0
Free R_{factor} (%)	25.6	23.1	25.0	24.0	23.0
RMS deviation					
Bond lengths (Å)	0.008	0.007	0.008	0.008	0.008
Bond angles (deg)	0.858	0.888	0.903	0.937	0.904

[a] $R_{sym} = \Sigma_{hkl} \Sigma_i | I_i - \langle I \rangle / \Sigma_{hkl} \Sigma_i \langle I \rangle$.
[b] $R_{factor} = \Sigma \| F_o | - | F_c \| / \Sigma | F_o |$.

cyanobacterial FNR system, in which the FNR is coupled transiently to Fld, is significant, and provides a good model for the FNR:Fld interaction.

The analysis of the structural models here reported, FNR mutants and FNR:Fld interaction, are discussed in the context of biochemical and structural data previously reported for this system.

MATERIALS AND METHODS

Crystallization and Data Collection

Crystals from K72E, K75R, K75Q, K75S, and K75E *Anabaena* FNR mutants were grown by the hanging drop method. Droplets with a volume of 5 μL, consisted of 2 μL of 0.75 mM protein solution buffered with 10 mM Tris-HCl pH 8.0, 1 μL of unbuffered β-octylglucoside at 5% (w/v), and 2 μL of reservoir solution containing 18–20% (w/v) polyethylene glycol 6000, 20 mM ammonium sulphate, and 0.1 M Mes-NaOH (pH 5.0–5.5). The droplets were equilibrated against a 1-mL reservoir solution at 20°C. Under these conditions, crystals grew within 1 to 7 days in the presence of phase separation caused by the detergent up to a maximum size of 0.7 × 0.4 × 0.4 mm. Cryoprotectant additives were tested to find suitable conditions to use cryo-techniques. Finally, crystals were soaked in a solution containing 70–75% of mother liquor and 25–30% glycerol for 1 min. A single crystal of each mutant was mounted in a loop and frozen at 100 K with a cryogenic system in a nitrogen stream. X-ray data were collected on a Mar Research (Germany) IP area detector using graphite monochromatic CuKα radiation generated by an Enraf-Nonius rotating anode generator to a maximum resolution of 2.3 Å. Synchrotron diffraction data were also collected from frozen crystals of K72E and K75E FNR mutants at 100 K on the D2AM beam line at ESRF (Grenoble), to a maximum resolution of 1.7 Å.

Crystals of all FNR mutants belong to the $P6_5$ hexagonal space group and the V_M is 3.0 Å^3/Da with one FNR molecule in the asymmetric unit and over 60% solvent content. All data sets were processed with MOSFLM[35] and scaled and reduced with SCALA from the CCP4 package (Collaborative Computational Project Number 4, 1994).

Three-Dimensional Structure Determination and Refinement

All the mutant structures were solved by molecular replacement using the program AMoRe[36] on the basis of the 1.8-Å resolution native FNR model[8] where the FAD cofactor, SO_4^{2-} and water molecules were removed. An unambiguous single solution for the rotation and translation functions was obtained for all proteins. These solutions were refined by the fast rigid body refinement program FITING.[37] The models were subjected to alternate cycles of conjugate gradient refinement with the program X-PLOR[38] by using the Engh and Huber force field at all times. The position of the mutated residues was shown clearly in the 2Fo − Fc density map and manual model building was done where necessary with the software package O.[39] At the later stages, water molecules were added. The resulting model was again subjected to more cycles of positional and B-factor refinement. Final models comprise residues 9–303 (the first eight residues were not observed in the electron density map), one FAD cofactor, one SO_4^{2-} molecule, and solvent molecules. Relevant refinement parameters are summarized in Table II. Atomic coordinates for all mutants have been deposited in the Protein Data Bank with codes 1GO2 for K72E, 1QGY

for K75E, 1E62 for K75R, 1E63 for K75S, and 1E64 for K75Q.

Modeling of the *Anabaena* FNR:Fld Complex

The CPR three-dimensional structure (PDB code 1AMO) has been used as a template to model the FNR:Fld interaction. This enzyme contains both FAD and FMN cofactors, and is composed of four structural domains. The FAD- and the NADP(H)-binding domains resemble the FNR three-dimensional structure and have been superimposed onto the *Anabaena* PCC7119 FNR coordinates (PDB code 1QUE), whereas the FMN-binding domain has been superimposed to the Fld structure from *Anabaena* PCC7120 (PDB code 1RCF). Both structural alignments have been performed by using the DALI server (http://www.ebi.ac.uk/dali/).[40]

RESULTS

Crystal Structures of the FNR Mutants at Position K75

The three-dimensional structures of the K75R, K75Q, K75S, and K75E *Anabaena* FNR mutants have been solved by X-ray crystallography. The overall three-dimensional folding for all these FNR forms results similarly to that reported for WT FNR, and only slight changes are present in the loop comprising residues 104 to 112. However, in all FNR structures so far reported a high mobility has been observed in this loop.[8,25] The residue at position 75 is well defined in all the mutant structures, and its side chain is exposed to the solvent.

The K75R conservative mutation does not disturb the positive charged character of the region, being that the charge distribution is very similar to that on the WT FNR surface (Fig. 2). This fact is in good agreement with previously reported biochemical data[30] showing that replacement of K75 by Arg resulted in the mutant with the most similar activity to the WT FNR (Table I). Although the structures solved for the K75Q and K75S FNR mutants show that replacement of Lys75 by either Gln or Ser does not produced an overall important alteration of the charge distribution on the FNR surfaces, the local positive charge is clearly absent around the 75 side-chain environment (Fig. 2). Consequently, this may explain why complex formation, and therefore subsequent ET, with the protein partners results are slightly hampered for these enzymes (Table I).[30] Finally, the electrostatic potential mapped onto the solvent-accessible surface of the K75E FNR structure shows that introduction of a Glu side chain at position 75 introduces a slight negative charge character in a mainly positively charged region (Fig. 2), providing an explanation to the large deleterious effect in the interaction and ET with Fld or Fd (Table I).[10] Although the K75E FNR three-dimensional structure does not show significant structural rearrangements in the backbone with respect to the WT FNR, replacement of K75 by Glu noticeably promotes the displacement of the K72 side chain from its position in WT FNR, leading to the formation of a new salt bridge interaction between E75 and K72 side chains [Fig. 3(A)].

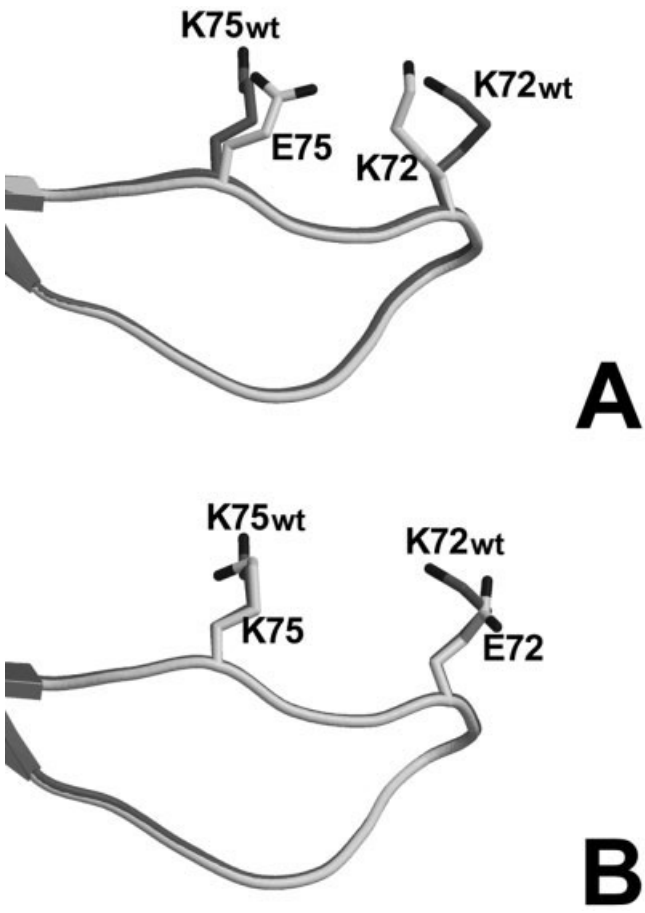

Fig. 3. Ribbon representation of the loop of *Anabaena* WT FNR containing residues 72 and 75, and the superposition of (A) K75E FNR and (B) K72E FNR. Side chains are shown as sticks. WT FNR is represented in dark gray and mutants in light gray.

The K75 side chain has been reported to modulate the protein/flavin interaction and to contribute to a long distance modulation of the flavin reduction potential within the protein environment. Thus, replacement of K75 by Glu results in a less negative reduction potential (by -20 mV) along with a weakening of the apoFNR:FAD interaction.[31] In the WT FNR crystal structure the K75 side chain is not making any contact with the FAD isoalloxazine and is not involved in any intramolecular interaction.[31] This feature is also observed in the structures of all the K75 mutants. However, position 75 is situated at the entrance of a cavity in which the pyrophosphate and the ribose from the FAD are situated. The structure of K75E does not show changes in the L conformation of FAD with regard to the WT, in contrast to previous hyphothesis.[31] However, slight different L conformers of FAD, producing less tight L conformers, are observed in the other mutants at the 75 position. Noticeably, the structure of K75E FNR shows that displacement of K75 side chain from the cavity to form a salt-bridge with K72 side chain is not accompanied by a displacement of the pyrophosphate and the ribose of FAD towards the cavity (not shown). Therefore, the mechanism by which position 75 in *Anabaena* FNR might influence the

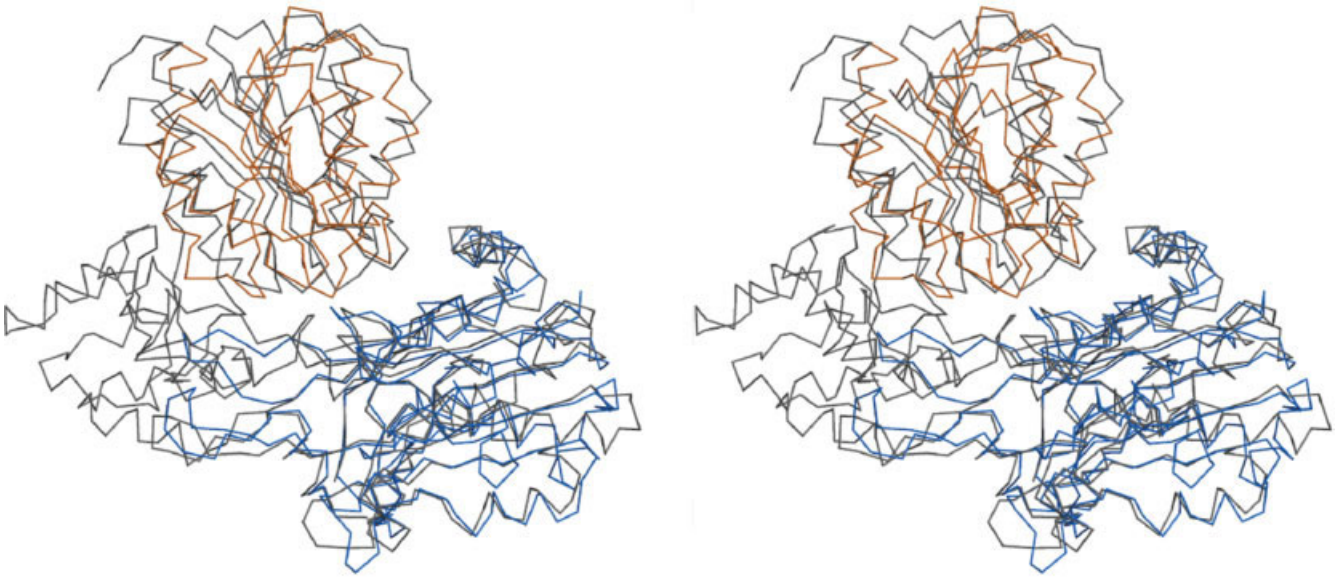

Fig. 4. Stereoview representation of the structural alignment of WT FNR (in blue) and WT Fld (in orange) onto CPR (in gray).

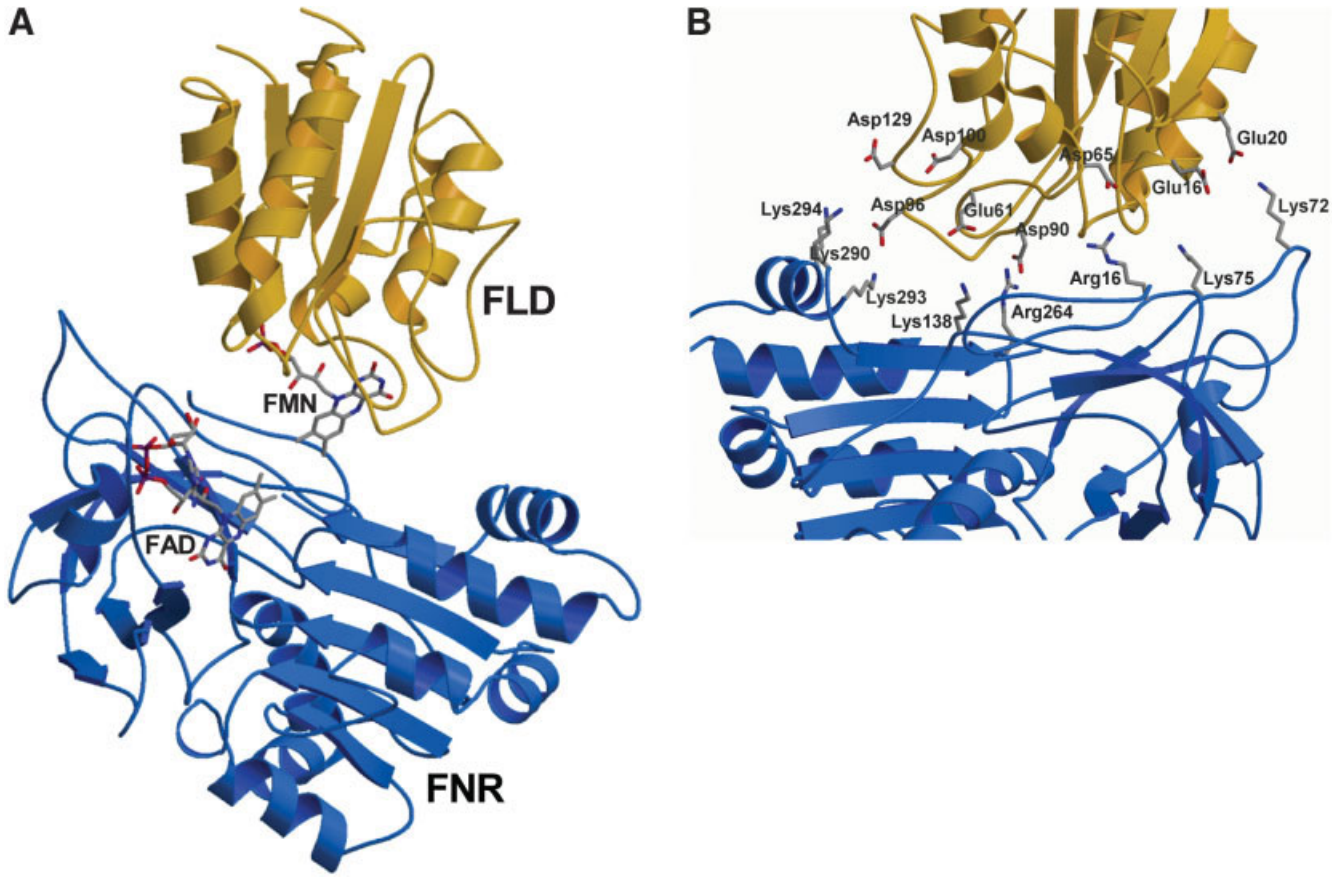

Fig. 5. (**A**) Putative FNR:Fld complex showing the relative position of FAD and FMN cofactors, (**B**) charged residues at the FNR:Fld interface. (**C**) Hydrophobic residues on FNR and Fld in the putative complex. In all representations, Fld is colored in yellow and FNR in blue. (**D**) Crystal structure of FNR:Fd complex (PDB code 1EWY) showing the relative position of the redox centers. (**E**) Charged residues at the FNR:Fd interface. (**F**) Hydrophobic residues on FNR and Fd in the crystal structure of the complex.

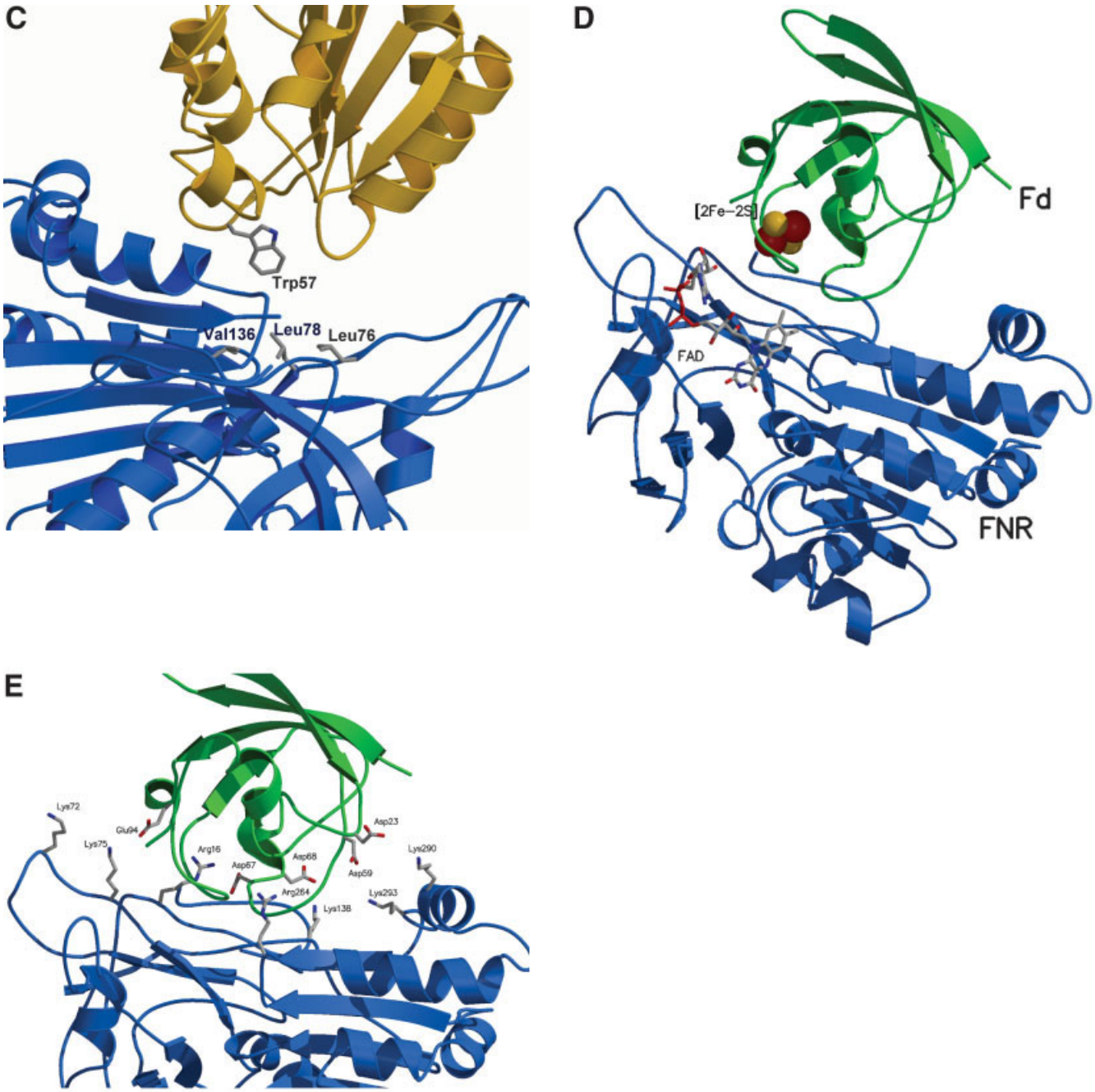

Figure 5. (Continued.)

flavin reduction potential still remains misunderstood. Nevertheless, differences in the water network connecting K75 side chain and the FAD pyrophosphate are found with all of the structures, suggesting a possible role for this side chain in the FAD properties propagated through the water molecules.

The Crystal Structure of the K72E FNR Mutant

The obtained three-dimensional structure for the K72E FNR mutant does not show significant rearrangements in the backbone, the overall structure being remarkably similar to that of WT FNR. The loop comprising residues 104–112 also presents a slightly different orientation in this mutant but, as explained above, this surely is a consequence of the high mobility of this loop.[8,25] Residues E72 and K75 are well defined and clearly exposed to the solvent in the electron density map of K72E FNR [Fig. 3(B)]. Taking as a reference the K75E FNR structure, an interaction between E72 and K75 in the K72E mutant could have been expected. However, the K72E FNR structure does not show any evidence of interaction between these two residues.

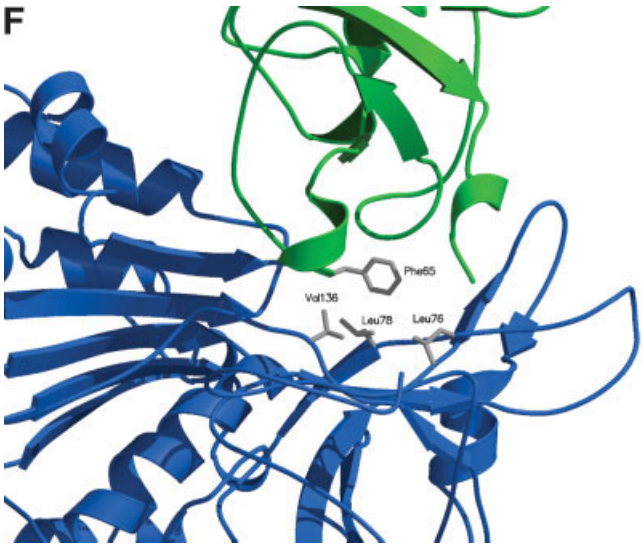

Figure 5. (Continued.)

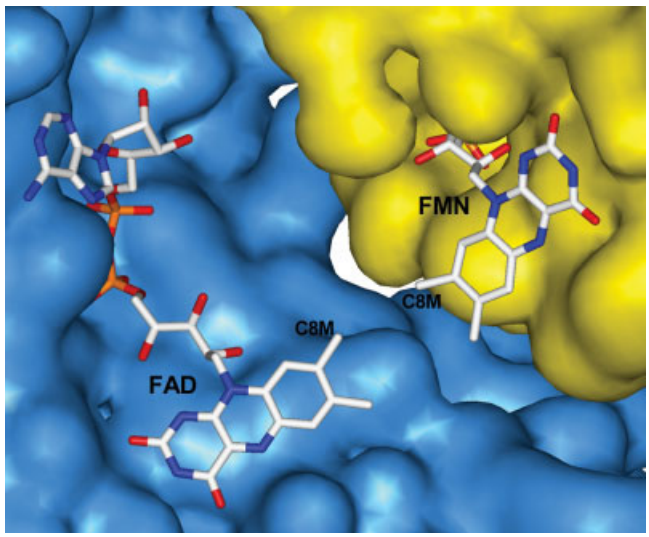

Fig. 6. Details of the interface for the putative FNR:Fld complex. No residues are present between both cofactors, making direct ET between them easy. FNR is colored in blue, Fld in yellow, and cofactors are in sticks representation.

Approach to a Three-Dimensional Model for the FNR:Fld Complex Structure

To get a deeper insight into the binding pattern of the FNR–Fld interaction, a model for the FNR:Fld interaction has been produced based on the structural superposition of FNR and Fld onto the multidomain CPR structure (Fig. 4). Although *Anabaena* FNR and the equivalent domain of CPR share only 26% of sequence identity, 274 residues (over 303) of FNR superimpose by structural alignment onto the FAD and NADP(H) binding domains of the rat CPR structure with a root-mean-squared deviation (RMSD) of 2.3 Å. Furthermore, the 21% sequence identity between *Anabaena* Fld and the CPR equivalent domain produces a structural superposition of 146 of the 168 Fld residues onto the Fld-like domain of CPR, again with an RMSD of 2.3 Å. These RMSD values clearly suggest that the structural superposition of FNR plus Fld onto the CPR structure is remarkably good, despite the fact that the FAD-and NADP(H)-binding domains of CPR are not contiguous in sequence.

Thus, the FNR:Fld model here proposed shows Fld binding on the concave side of FNR, around the FAD cofactor and mainly interacting with the FAD binding domain of FNR [Fig. 5(A)], with the interface between both proteins clearly complementary [Figs. 5(B) and (C)]. Several positively charged residues on the FNR surface are situated in front of negatively charged ones on the Fld surface, suggesting formation of several ion pairs [Fig. 5(B), Table III). Thus, all positively charged residues previously proposed by biochemical studies to be involved in an FNR:Fld complex formation, namely R16, K72, K75, R264, K290,[2,10] are lying within the interaction surface between both proteins. Possible ionic pairs formed at the FNR:Fld interface are given in Table III and compared with those found in the crystal structure of the *Anabaena* FNR:Fd complex (PDB code 1EWY) [Figs. 5(D–F)]. It is worth noting that the orientation of charged residues in both redox partners, Fd and Fld, within the FNR complexes is consistent with the previously reported alignment between Fd and Fld reported by Ullman,[34] on the basis of their electrostatic potentials.

Careful observation of the complex interface suggests that not only electrostatic but also hydrophobic interactions stabilize the complex. Hydrophobic patches located on the FNR and Fld surfaces in the close environment of their FAD and FMN cofactors seem to contribute to the stabilization of the FNR:Fld interaction [Fig. 5(C)]. Thus, in our model the side chains of residues L76, L78, and V136 of FNR, previously shown as key side chains for the formation of optimal complexes with either Fd or Fld,[26,27] would be stabilized by the interaction with the Fld W57 side chain. Additionally, superposition of our model onto the FNR:Fd three-dimensional structure clearly shows that Fld W57 superimposes with Fd F65 in the FNR:Fd complex [Fig. 5(F)], a key residue in the processes of Fd,[20] thus suggesting a similar role for both residues. Noticeably, in *Anabaena* Fld W57, has been shown to play an important role in setting the structural and electronic environment to allow efficient ET from PSI to FNR.[44]

Additionally, molecular dipoles for FNR and Fld in the FNR:Fld model, as calculated by GRASP,[42] are nearly collinear and orientated in the same direction (not shown). This disposition is identical to that exhibited by the crystal structure of the FNR:Fd complex.[11] Finally, the model shows a different relative disposition of the FAD and FMN redox centers in comparison to that observed between FAD and [2Fe-2S] in the FNR:Fd complex. Thus, although in the FNR:Fd complex the minimal distance between the C8-isoalloxazine methyl group (C8M) of the FAD cofactor (the putative place for ET[11,43]) and the [2Fe-S] cluster of Fd is 7.4 Å, in the FNR:Fld model, the FAD C8M would separate only 4.1 Å from the FMN C8M (Fig. 6). Such a small distance might be adequate for direct ET between

TABLE III. Electrostatic and Hydrophobic Interactions between FNR and Fld (Proposed Model) or Fd (PDB Code 1EWY)

FNR residues	Fld residues	Fd residues
Electrostatic interactions		
R16	D65	D67
K72	E20	—
K75	E16,E20	E94
K138	D61, D67	D68
R264	D90	—
K290	D96, D129	D23
K293	D96	D59
Hydrophobic interactions		
L76	W57	F65
L78	W57	F65
V136	W57	—

TABLE IV. NADPH-Dependent Cytochrome *c* Reductase Activity of FNR with Different Mutated Flavodoxins as the Mediator[a]

Fld form	k_{cat}^{Fld} (s^{-1})	K_m^{Fld} (μM)	k_{cat}/K_m^{Fld} ($\mu M^{-1}s^{-1}$)	K_d (μM)
WT[a]	23.3	33.0	0.70	3.0
E16Q	15.0	94.0	0.16	20.8
E20K	25.0	172.0	0.14	14.5
E61A	19.3	144.6	0.13	15.0
E61K	31.3	166.3	0.19	11.4
D65K	15.1	20.0	0.75	5.9
D96N	11.0	11.1	0.99	19.4

[a]Taken from Ref. [45].

the two prosthetic groups. Additionally, upon complex formation a wide cavity appears between the cofactors in which no residue precludes direct ET between the two redox centers.

DISCUSSION

The three-dimensional structure of the FNR displays several positively charged side chains on its surface situated around the FAD cofactor, suggesting a function for such residues in the protein partner recognition.[2,43] Matching this observation, Fd and Fld structures show acidic patches on their surfaces. Characterization of charge-reversed mutants has confirmed that electrostatic binding forces are predominant in the initial stages of recognition and complex formation between FNR and its protein electron donors.[10,20–22,30,31] Additionally, site-directed mutagenesis studies also suggest that hydrophobic interactions are involved in the rearrangement of the initial interaction to produce the optimal complex for ET.[2,26,27] Analysis on the *Anabaena* system also indicates that very specific interactions, both electrostatic and hydrophobic, between FNR and Fd surface side chains are required for an efficient interaction, whereas the FNR:Fld system might present less geometric requirements for an efficient ET.[2] In this study we have tried to further understand the role of electrostatic interactions in the FNR:Fld and FNR:Fd interactions from a structural point of view by modeling the FNR:Fld interaction at the same time that we try to understand from the structural point of view the effects observed upon mutation of K72 and K75 in FNR in the interaction with Fd and Fld. Previous site-directed mutagenesis studies proved that among all positively charged residues around the FAD cofactor of FNR, K72 and, especially, K75 side chains are key for the interaction between FNR and the protein partners.[10,30] Thus, whereas K75 is essential for recognition of both Fd and Fld, K72 influences mainly Fld binding (Table I). The obtained three-dimensional structures here reported for the K75R, K75Q, and K75S FNR mutants do not show major structural rearrangements either in global FNR structure or in the loop that comprises position 75. However, the K75E mutant displays a new orientation of K72 side chain, allowing establishment of a salt bridge between both residues [Fig. 3(A)]. Therefore, analysis of the three-dimensional structure of the K75E FNR as presented here indicates that in this mutant two-key FNR positively charged residues result in simultaneously disabling complex formation with the protein partner, giving an explanation for the remarkable decrease in binding and ET abilities observed for the K75E mutant.[30] Contrarily, K72E FNR does not show any local arrangement that allows interaction with K75. Therefore, the larger structural arrangements observed in the K75E mutants might explain the fact that the K72E mutant is able to transfer electrons to either Fd and Fld, whereas K75E does not show either binding or ET abilities to either Fd or Fld (Table I). However, analysis of the FNR:Fld structure would make the understanding of this point easier.

The lack of an FNR:Fld complex structure also makes it difficult to identify and compare residues with a similar function in Fld to those so far reported in Fd for FNR recognition and ET. However, the three-dimensional structure of CPR could help us to partially overcome this problem.[33] CPR is a four-domain enzyme, comprising an FMN-binding domain, a connecting domain, an FAD-binding domain, and an NADPH-binding domain, which belongs to the FNR structural family. The CPR FMN-binding domain is superimposable to Fld, whereas FNR is the structural prototype that includes the FAD and NADPH-binding domains of CPR. Additionally, the different domains of CPR play a similar function than Fld + FNR in the photosynthetic chain, by exchanging electrons between pyridine nucleotides and FMN, via an FAD group. Therefore, the crystallographic structure of CPR seems a good template to model the interaction between *Anabaena* Fld and FNR. Our FNR:Fld model shows several putative electrostatic and hydrophobic interactions between FNR and Fld (Table III and Fig. 5). Noticeably, the electrostatic interactions are not found in the CPR structure, because these proteins do not present charged residues at the equivalent positions than FNR and Fld. This is easy to understand because its domains are already at the adequate distance for ET and do not need to find each other to form a complex prior to ET. All residues on FNR that are found interacting with Fd in the three-dimensional structure reported for the FNR:Fd complex present equivalent

interactions in our FNR:Fld model. Additionally, it is shown that FNR might form a larger number of interactions with Fld than with Fd, by either involving more residues on the Fld surface (K72, K138, V136, R264) and/or by additional interactions with a single residue (K75, K138, K290) (Table III). This would explain why some of these residues have been shown as determinant for an efficient interaction with Fld, but are not so critical in the interaction with Fd (Table I).[10] Formation of the FNR:Fld complex implies a higher interface between both proteins than in the FNR:Fd one, due to the larger Fld size. In this new interaction surface, K72, R264, andV136 of FNR can be included, thus explaining why mutation of these residues has more repercussion in the FNR ET with Fld than with Fd. K75 is situated within the interface at an adequate distance from Fld E16 and E20 side chains to interact during complex formation, as reported for K75 with Fd E94 in the crystal structure for the FNR:Fd complex.[11] Therefore, the structure of the K75E mutant presented here is in agreement with the fact that replacement of K75 by glutamate impairs FNR:Fld and FNR:Fd complex formation by preventing these salt bridge formations.[30] Moreover, our model also shows possible hydrophobic interactions between residues L76, L78, and V136 from FNR with W57 from Fld, suggesting a similar role for W57 in Fld and F65 in Fd. The key role of L76 and L78 on FNR in Fd and Fld recognition has been experimentally proven in the processes of interaction and electron transfer, as well as the role played by an aromatic residue at position 57 of *Anabaena* Fld.[44] Recent site-directed mutagenesis studies on negatively charged residues on Fld surface indicate that E16, E20, E61, D65, and D96 contribute to the orientation and optimization of the Fld interaction, either with FNR or with PSI, for efficient ET.[45] This is consistent with the model presented here, which suggests that all these residues are involved in salt bridges with FNR side chains. However, these data also indicate that none of these side chains are involved in the formation of crucial interactions for optimal interaction with FNR, because all the mutants retain part of Fld abilities to bind and to exchange electrons with FNR. Thus, these recent reported data support the idea that the FNR/Fld interaction is less specific than the FNR/Fd one.[45] Finally, analysis of this putative FNR:Fld interactions also raised another interesting point on the processes of ET between proteins. The model clearly shows that ET between FAD and FMN might take place to a much shorter distance than in the case of FNR and Fd redox centers, suggesting that probably only the flavin atoms will be directly responsible for ET, and that Fld could orientate in different ways on the FNR surface without significantly altering the distance between the methyl groups of FAD and FMN. If the main requirement for ET is the proximity of the redox centers in a nonpolar environment, this might explain why mutagenesis of the individual residues has not revealed one that is critical for the efficient interaction with FNR, and why subtle changes in the Fld surface electrostatic potential and dipole moment still produce complexes that allow ET. Therefore, Table III summarizes possible ionic and hydrophobic interactions deduced from the model presented here, but it is feasible that other interactions could also be produced upon complex formation.

CONCLUSIONS

Three-dimensional structures for five FNR mutants have been obtained as well as a model of the FNR:Fld interaction. Formation of an intramolecular salt bridge between K72 and E75 in *Anabaena* K75E FNR structure is reported. This might explain the lost of activity exhibited by this mutant, and confirms the importance of positive charges at positions 75 and 72 in FNR for Fd and Fld recognition. The model proposed for the FNR:Fld interaction suggests the involvement of a larger FNR surface than in the interaction with Fd and an adequate distance for ET between redox centers without intermediate groups. Analysis of this model in the light of previous biochemical and structural data suggest that it represents a good approach to advance in the knowledge of complex formation and subsequent ET between FNR and Fld until crystal structure of the FNR:Fld is available.

REFERENCES

1. Carrillo N, Ceccarelli EA. Open questions in ferredoxin-NADP$^+$ reductase catalytic mechanism. Eur J Biochem. 2003;270:1900–1915.
2. Medina M, Gómez-Moreno C. Interaction of ferredoxin-NADP$^+$ reductase with its substrates: optimal interaction for efficient electron transfer. Photosynthesis Res 2004;79:113–131.
3. Sykes GA, Rogers LJ. Redox potentials of algal and cyanobacterial flavodoxins. Biochem J 1984;217:845–850.
4. Fillat MF, Edmondson DE, Gomez-Moreno C. Structural and chemical properties of a flavodoxin from *Anabaena* PCC 7119. Biochim Biophys Acta 1990;1040:301–307.
5. Karplus PA, Daniels MJ, Herriott JR. Atomic structure of ferredoxin-NADP$^+$ reductase: prototype for a structurally novel flavoenzyme family. Science 1991;251:60–66.
6. Correll CC, Batie CJ, Ballou DP, Ludwig ML. Phthalate dioxygenase reductase: a modular structure for electron transfer from pyridine nucleotides to [2Fe-2S]. Science 1992;258:1604–1610.
7. Karplus PA, Bruns M. Structure–function relations for ferredoxin reductase. J Bioenerg Biomembr 1994;26:89–99.
8. Serre L, Vellieux FMD, Medina M, Gómez-Moreno C, Fontecilla-Camps JC, Frey M. X-ray structure of the ferredoxin:NADP$^+$ reductase from the cyanobacterium *Anabaena* PCC 7119 at 1.8 Å resolution, and crystallographic studies of NADP$^+$ binding at 2.25 Å resolution. J Mol Biol 1996;263:20–39.
9. Jelesarov I, De Pascalis AR, Koppenol WH, Hirasawa M, Knaff DB, Bosshard R Ferredoxin binding site on ferredoxin: NADP$^+$ reductase. Differential chemical modification of free and ferredoxin-bound enzyme. Eur J Biochem 1993;216:57–66.
10. Martínez-Júlvez M, Medina M, Gómez-Moreno C. Ferredoxin-NADP(+) reductase uses the same site for the interaction with ferredoxin and flavodoxin. J Biol Inorg Chem 1999;4:568–578.
11. Morales R, Kachalova G, Vellieux F, Charon MH, Frey M. Crystallographic studies of the interaction between the ferredoxin-NADP$^+$ reductase and ferredoxin from the cyanobacterium *Anabaena*: looking for the elusive ferredoxin molecule. Acta Crystallogr D Biol Crystallogr 2000;56:1408–1412.
12. Morales R, Charon MH, Hudry-Clergeon G, Petillot Y, Norager S, Medina M, Frey M. Refined X-ray structures of the oxidized, at 1.3 Å, and reduced, at 1.17 Å, [2Fe-2S] ferredoxin from the cyanobacterium *Anabaena* PCC7119 show redox-linked conformational changes. Biochemistry 1999;38:15764–15773.
13. Rao ST, Shaffie F, Yu C, Satyshur KA, Stockman BJ, Markley JL, Sundaralingam M. Structure of the oxidized long-chain flavodoxin from *Anabaena* 7120 at 2 Å resolution. Protein Sci 1992;1:1413–1427.
14. Zanetti G, Gozzer C, Sacchi G, Curti B. Modification of arginyl

residues in ferredoxin-NADP$^+$ reductase from spinach leaves. Biochim Biophys Acta 1979;568:127–134.
15. Zanetti G, Aliverti A, Curti B. A cross-linked complex between ferredoxin and ferredoxin-NADP$^+$ reductase. J Biol Chem 1984; 259:6153–6157.
16. Batie CJ, Kamin H. Ferredoxin:NADP$^+$ oxidoreductase. Equilibria in binary and ternary complexes with NADP$^+$ and ferredoxin. J Biol Chem 1984;259:8832–8839.
17. Batie CJ, Kamin H. Electron transfer by ferredoxin:NADP$^+$ reductase. Rapid-reaction evidence for participation of a ternary complex. J Biol Chem 1984;259:11976–11985.
18. Medina M, Mendez E, Gómez-Moreno C. Identification of arginyl residues involved in the binding of ferredoxin-NADP$^+$ reductase from *Anabaena* sp. PCC 7119 to its substrates. Arch Biochem Biophys 1992;299:281–286.
19. Medina M, Mendez E, Gómez-Moreno C. Lysine residues on ferredoxin-NADP$^+$ reductase from *Anabaena* sp. PCC 7119 involved in substrate binding. FEBS Lett 1992;298:25–28.
20. Hurley JK, Salamon Z, Meyer TE, Fitch JC, Cusanovich MA, Markley JL, Cheng H, Xia B, Chae YK, Medina M, Gómez-Moreno C, Tollin G. Amino acid residues in *Anabaena* ferredoxin crucial to interaction with ferredoxin-NADP$^+$ reductase: site-directed mutagenesis and laser flash photolysis. Biochemistry 1993;32:9346–9354.
21. Hurley JK, Medina M, Gómez-Moreno C, Tollin G. Further characterization by site-directed mutagenesis of the protein–protein interface in the ferredoxin/ferredoxin:NADP$^+$ reductase system from *Anabaena*: requirement of a negative charge at position 94 in ferredoxin for rapid electron transfer. Arch Biochem Biophys 1994;312:480–486.
22. Hurley JK, Hazzard JT, Martínez-Júlvez M, Medina M, Gómez-Moreno C, Tollin G. Electrostatic forces involved in orienting *Anabaena* ferredoxin during binding to *Anabaena* ferredoxin: NADP$^+$ reductase: site-specific mutagenesis, transient kinetic measurements, and electrostatic surface potentials. Protein Sci 1999;8:1614–1622.
23. Aliverti A, Corrado ME, Zanetti G. Involment of lisin-88 of spinach ferredoxin-NADP$^+$ reductase in the interaction with ferredoxin. FEBS Lett 1994;343:247–250.
24. Jelesarov I, Bosshard HR. Thermodynamics of ferredoxin binding to ferredoxin:NADP$^+$ reductase and the role of water at the complex interface. Biochemistry 1994;33:13321–13328.
25. Martínez-Júlvez M, Hermoso JA, Hurley JK, Mayoral T, Sanz-Aparicio J, Tollin G, Gómez-Moreno C, Medina M. Role of Arg100 and Arg264 from *Anabaena* PCC 7119 ferredoxin-NADP$^+$ reductase for optimal NADP$^+$ binding and electron transfer. Biochemistry 1998;37:17680–17691.
26. Martínez-Júlvez M, Nogués I, Faro M, Hurley JK, Brodie TB, Mayoral T, Sanz-Aparicio J, Hermoso JA, Stankovich MT, Medina M, Tollin G, Gómez-Moreno C. Role of a cluster of hydrophobic residues near the FAD cofactor in *Anabaena* PCC 7119 ferredoxin-NADP$^+$ reductase for optimal complex formation and electron transfer to ferredoxin. J Biol Chem 2001;276:27498–27510.
27. Nogués I, Martinez-Julvez M, Navarro JA, Hervas M, Armenteros L, de la Rosa MA, Brodie TB, Hurley JK, Tollin G, Gomez-Moreno C, Medina M. Role of hydrophobic interactions in the flavodoxin mediated electron transfer from photosystem I to ferredoxin-NADP$^+$ reductase in *Anabaena* PCC 7119. Biochemistry 2003;42: 2036–2045.
28. Hurley JK, Cheng H, Xia B, Markley JL, Medina M, Gómez-Moreno C, Tollin G. An aromatic amino acid is required at position 65 in *Anabaena* ferredoxin for rapid electron transfer to ferredoxin-NADP$^+$ reductase. J Am Chem Soc 1993;115:11698–11701.
29. Gómez-Moreno C, Martínez-Júlvez M, Medina M, Hurley JK, Tollin G. Protein–protein interaction in electron transfer reactions: the ferredoxin/flavodoxin/ferredoxin:NADP$^+$ reductase system from *Anabaena*. Biochimie 1998;80:837–846.
30. Martínez-Júlvez M, Medina M, Hurley JK, Hafezi R, Brodie T, Tollin G, Gómez-Moreno C. Lys75 of *Anabaena* ferredoxin-NADP$^+$ reductase is a critical residue for binding ferredoxin and flavodoxin during electron transfer. Biochemistry 1998;37:13604–13613.
31. Faro M, Gómez-Moreno C, Stankovich M, Medina M. Role of critical charged residues in reduction potential modulation of ferredoxin-NADP$^+$ reductase. Eur J Biochem 2002;269:2656–2661.
32. Kurisu G, Kusunoki M, Katoh E, Yamazaki T, Teshima K, Onda Y, Kimata-Ariga Y, Hase T. Structure of the electron transfer complex between ferredoxin and ferredoxin-NADP(+) reductase. Nat Struct Biol 2001;8:117–121.
33. Wang M, Roberts DL, Paschke R, Shea TM, Masters BS, Kim JJ. Three-dimensional structure of NADPH-cytochrome P450 reductase: prototype for FMN- and FAD-containing enzymes. Proc Natl Acad Sci USA 1997;94:8411–8416.
34. Ullmann GM, Hauswald M, Jensen A, Knapp EW. Structural alignment of ferredoxin and flavodoxin based on electrostatic potentials: implications for their interactions with photosystem I and ferredoxin-NADP$^+$ reductase. Proteins Struct Funct Genet 2000;38:301–309.
35. Leslie AGW. In: Helliwell JR, Machin PA, Papiz MZ, editors. Proceedings of the CCP4 study weekend. Warrington, UK: SERC Daresbury; 1987. p 39–50.
36. Navaza J. AMoRe: an automated package for molecular replacement. Acta Crystallogr A 1994;50:157–163.
37. Castellano E, Oliva G, Navaza, J. Fast rigid-body refinement for molecular-replacement techniques. J Appl Crystallogr 1992;25: 281–284.
38. Brünger AT X-PLOR: a system for X-ray crystallography and NMR. New Haven, CT: Yale University Press; 1993.
39. Jones TA, Zou JY, Cowan W, Kjeldgaard M. Improved methods for building protein models in electron density maps and the location of errors in these models. Acta Crystallogr 1991;A47:110–119.
40. Holm L, Sander C. Protein structure comparison by alignment of distance matrices. J Mol Biol 1993;233:123–138.
41. Schmitz S, Martínez-Júlvez M, Gómez-Moreno C, Böhme H. Interaction of positively charged amino acid residues of recombinant, cyanobacterial ferredoxin:NADP$^+$ reductase with ferredoxin probed by site directed mutagenesis. Biochim Biophys Acta 1998;1363:85–93.
42. Nicholls A, Bharadwj R, Honig B. GRASP: graphical representations and analysis of surface properties Biophys J 1993;64:166.
43. Knaff DB, Hirasawa M. Ferredoxin-dependent chloroplast enzymes. Biochim Biophys Acta 1991;1056:93–125.
44. Casaus JL, Navarro JA, Hervas M, Lostao A, De la Rosa MA, Gomez-Moreno C, Sancho J, Medina M. *Anabaena* sp. PCC 7119 flavodoxin as electron carrier from photosystem I to ferredoxin-NADP$^+$ reductase. Role of Trp(57) and Tyr(94). J Biol Chem 2002;277:22338–22344.
45. Nogués I, Hervás M, Peregrina JR, Navarro JA, de la Rosa MA, Gómez-Moreno C, Medina M. *Anabaena* flavodoxin as electron carrier from photosystem I to ferredoxin-NADP$^+$ reductase. Role of flavodoxin residues in protein–protein interaction and electron transfer. Biochemistry 2005;44:97–104.
46. Medina M, Martinez-Julvez M, Hurley JK, Tollin G, Gomez-Moreno C. Involvement of glutamic acid 301 in the catalytic mechanism of ferredoxin NADP+ reductase from *Anabaena* PCC 7119. Biochemistry 1998;37:2715–2728.